

Search for general relativistic effects in table-top displacement metrology

Peter G. Halverson, Daniel R. Macdonald, Rosemary T. Diaz
 Jet Propulsion Laboratory, California Institute of Technology
 4800 Oak Grove Drive, Pasadena CA, 91109
 peter.halverson@jpl.nasa.gov

Abstract: As displacement metrology accuracy improves, general relativistic effects will become noticeable. Metrology gauges developed for the Space Interferometry Mission, were used to search for locally anisotropic space-time, with a null result at the 10^{-10} level.

©2003 Optical Society of America

OCIS codes: (120.3940) Metrology (120.3180) Interferometry (000.2780) Gravity

I. Extended Abstract

1. Introduction

General relativity predicts that remotely referenced displacement metrology [1] will experience an error accumulating at $(dL/L)/dh=0.00011$ pm/m² of altitude difference. *E.g.*, a standard at JPL (~400 m altitude) will appear 0.15 pm longer to a client at Mount Wilson (~1800 meters). Verifying effects like this and searching for exotic effects predicted by alternative theories has the potential to discover “new physics.” We describe a search for anisotropy due to the gravitational field of the sun suggested by Tomozawa [2], using pre-existing apparatus.

2. Experiment

NASA/JPL’s Space Interferometry Mission (SIM) [3,4] has motivated the development of interferometric heterodyne displacement metrology gauges with repeatability roughly 50 pm[5]. The gauges’ linearity and thermal stability are tested [6] in a temperature stabilized vacuum tank with a dedicated laser source, a temperature stabilized 1.3 micron YAG coupled to two AOMs to produce two frequencies separated by 2 kHz. This experiment used two gauges: A oriented east-west and B north-south, monitoring the distance between corner-cube retroreflectors separated by 76 +/- .2 cm. A feedback system [7] maintained head alignment with the retroreflectors. Equal length baselines made the effect of laser frequency drift common to both gauges, making it straightforward to search for anisotropies. *E.g.*, a non-isotropic metric would be observed as change in the A-B length difference.

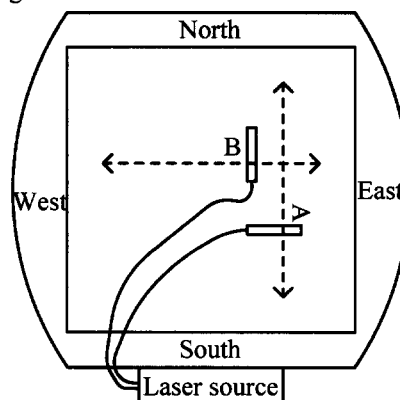


Figure 1. Laser source and optical bench in thermally isolated vacuum chamber. Metrology heads A and B were supplied by a common source via optical fibers and monitored the 76 cm E-W and N-S baselines.

3. Results

Displacement and alignment data for both gauges, and system temperatures were recorded at 6 points/hour from Dec 24, 2002 to Jan 23, 2003. Figure 2 shows the relative length difference (A-B) for this period. Features such as the initial drop, 290 pm/hour rise and dip closely follow the temperature of the aluminum optical table in the tank, indicating a slight thermal-optic asymmetry. After removing the linear trend and applying a Hanning filter, the Fourier amplitudes of the (A-B) data were computed (figure 3).

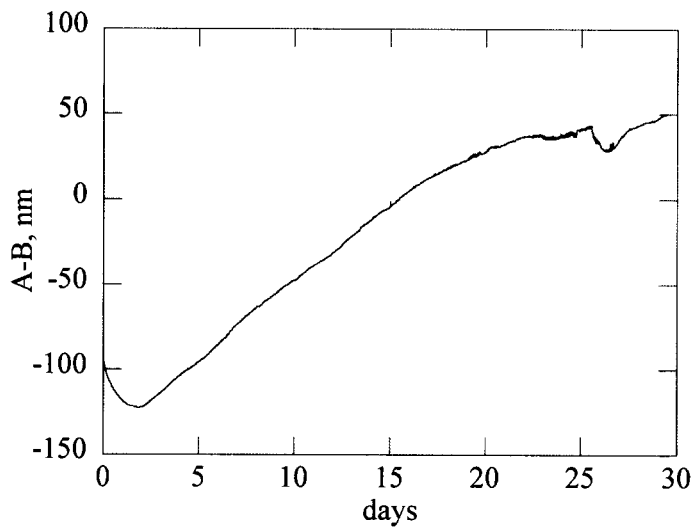


Figure 2. Length difference A-B.

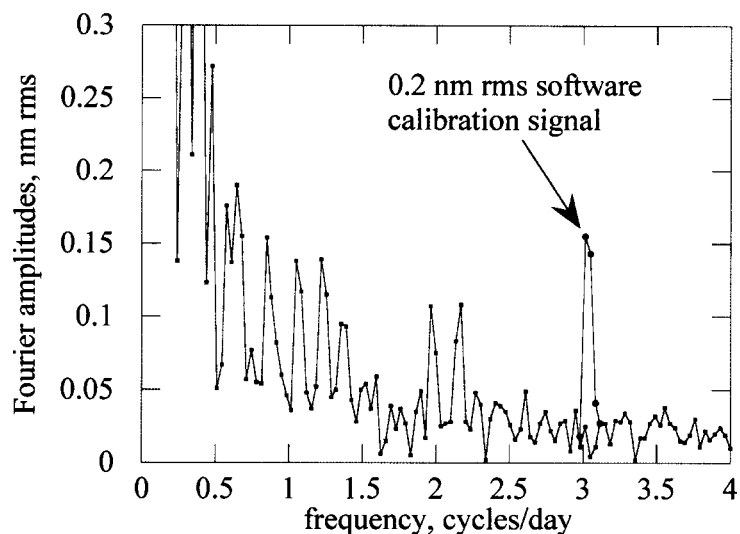


Figure 3. Frequency spectrum of A-B, normalized so peak height indicates RMS amplitude. *E.g.*, the points in the 3 cpd test signal add (in quadrature) to 0.2 nm.

4. Interpretation.

The data rule out the original motivation for this work: the possibility of an anisotropy order $M_{\text{SUN}}G/(c^2R)$, $R=1$ AU, correlated with sun direction. Such an effect, which would create a nm amplitude peak at 2 cpd, can be ruled out at the 0.1 nm level. Other interesting frequencies to examine are the sidereal day (1.0027 and 2.0055 cpd) and the moon's apparent position (0.966 and 1.932 cpd, the tide frequency). Testing frequencies around 1 cpd is problematic because of diurnal effects such as temperature changes. However at 2 cpd, things are more interesting. The 130 pm peak at 1.93 cpd might be tidal effects: ground tilt, movement of vacuum tank, but the peak at 2.13 cpd is not easily explained. Neither peak is in the temperature or pointing data, ruling out these obvious explanations.

5. Conclusion

A “parasitic” Michelson-Morley like experiment was conducted, ruling out local 10^{-10} anisotropies. Although this limit is not competitive with recent results [8], the experiment proved interesting and helps validate SIM metrology. A possible correlation with the lunar period hints at a local “tidal” effect.

II. Further Discussion

1. Motivation

The experiment described above was motivated by the suggestion by Tomozawa [2] that certain general relativistic (G.R.) effects may have been overlooked, that existing SIM metrology testbeds might have a chance to see something interesting. However, results by the “COREs” group [8,9] set a much more stringent limit of a few $\times 10^{-15}$ for local anisotropies, several orders of magnitude better than what could be done in this work. Nevertheless, independent tests are useful, and it is interesting to note that (non-local) anisotropies due to the sun's gravitation field *are* observed in the “metrology” of distances to interplanetary spacecraft [10,11]. These effects are of order 10^{-7} (for solar limb grazing Earth-Mars ranging) but it should be emphasized that they are predicted by G.R. and do not represent “new physics”.

This work also represents a snapshot of the metrology capabilities of the Space Interferometry Mission at the end of 2002. The 150 nm drift in 25 days, or 250 pm/hour drift rate demonstrate that we are close to but not quite at SIM's required stability of ~50 pm/hour.

2. Testbed reconfiguration

For the anisotropy search, the SIM Two-Gauge test facility (see Appendix) gauges were repositioned to have perpendicular beams, and additional fiducials were added on the north and south ends of the breadboard (figure 1). The facility reconfigured for the experiment is shown in fig. 4.

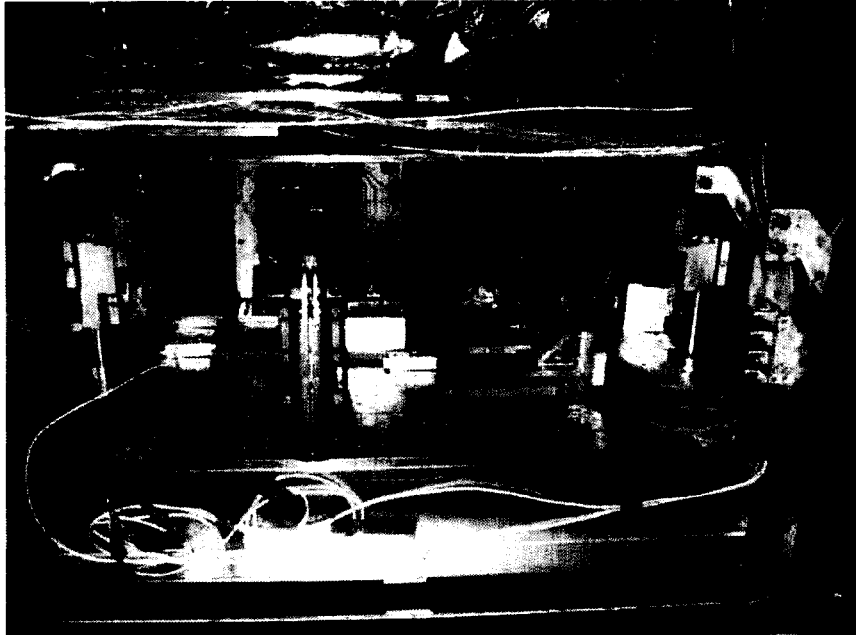


Fig. 4. View inside vacuum chamber. Laser metrology beam A travels between corner-cube fiducials visible atop posts at the left and right ends of the breadboard. Beam B travels between the corner cube atop the pillar at the near edge of the bread board and another (not visible) at the rear. The beams originate from the metrology heads mounted between the fiducials.

For thermal stability, the system was warmed to slightly above room temperature (to recover from the pump-down cold-shock) and allowed to thermally drift. The vacuum tank was held at 20 ± 0.03 C.

3. Search for extraneous effects.

The metrology system is sensitive to factors including

- Temperature induced expansion of the metrology heads, and in this experiment, gradients in the breadboard.
- Temperature induced drift in laser wavelength, coupled with imperfect matching of the two orthogonal distances.
- “Creep”, or slow deformation of the materials used in the metrology heads, and in this experiment, of the mechanics holding the corner-cube fiducials.
- Errors in pointing the metrology beams to the fiducials.

Temperature of metrology heads, breadboard

A plot of east-west vs. north-south distance difference, together with temperature difference of the metrology heads, shows a correlation, fig. 5. This was expected as the metrology heads have a known ~8 nm/K temperature coefficient.

However, the experiment is well decoupled from laboratory temperature variations, and in particular, there are no components near the 2 cycles per day region of interest for G.R. See fig. 6.

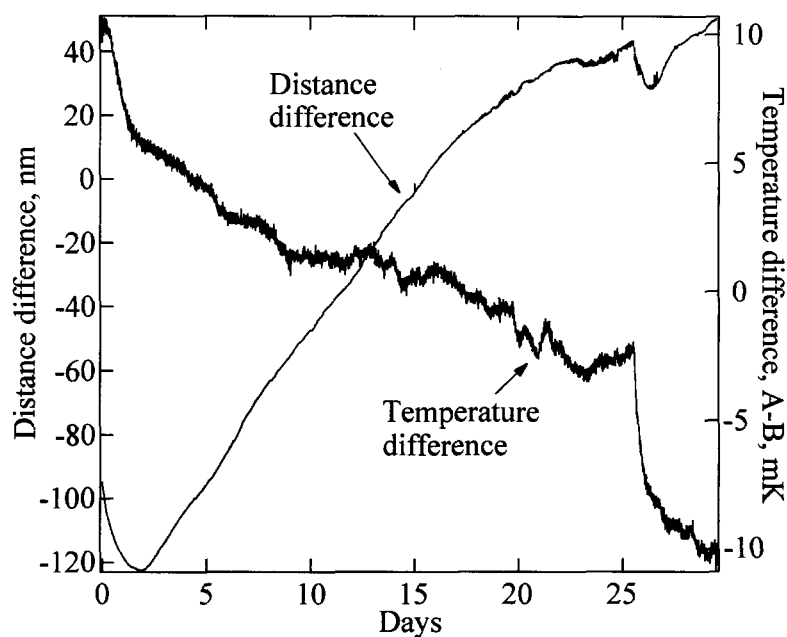


Fig. 5. Time series of distance difference and metrology head temperature difference.

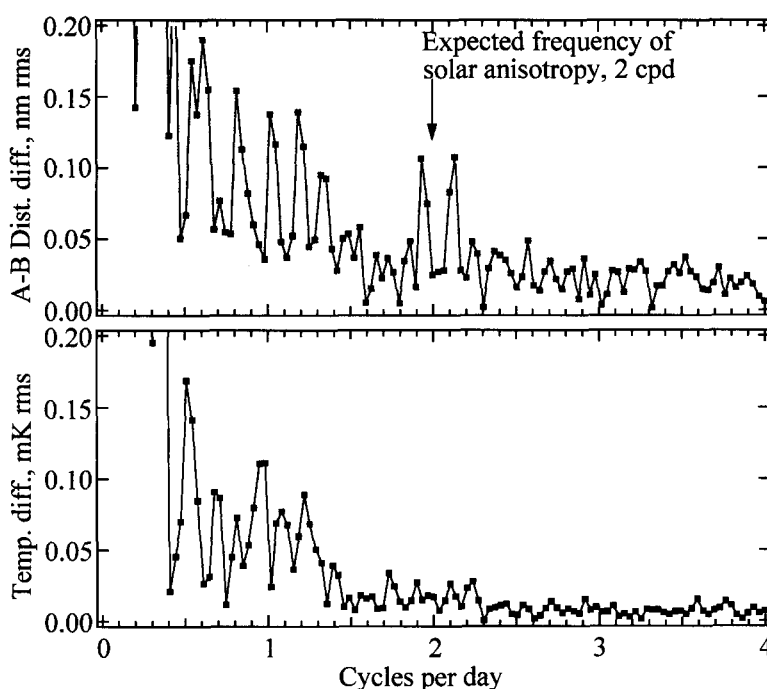


Fig. 6. Fourier amplitudes of distance difference and temperature difference.

Temperature of laser

The laser temperature was held constant to ± 0.1 C and no significant correlation between the residual temperature fluctuations and distance difference could be found.

Creep

Some of the gradual change in measured distance is attributable to creep (slow change in shape) of the optical mounts. A suspected cause is a teflon retaining ring holding the beam splitter in figure 11.

Pointing Drift

Because of the automatic alignment mechanism, the metrology gauges never became measurably mispointed. (Any measurable mispointing would be removed by the feedback loop.) However it is interesting to look at the correction signal applied to the PZT actuators, fig. 7.

Both gauges exhibit a slow trend explainable by temperature drift, and sudden "events". We again suspect instability of the teflon-mounted beam splitter. However the frequency spectrum of the pointing control data has no components near the 2 cycles per day region of interest.

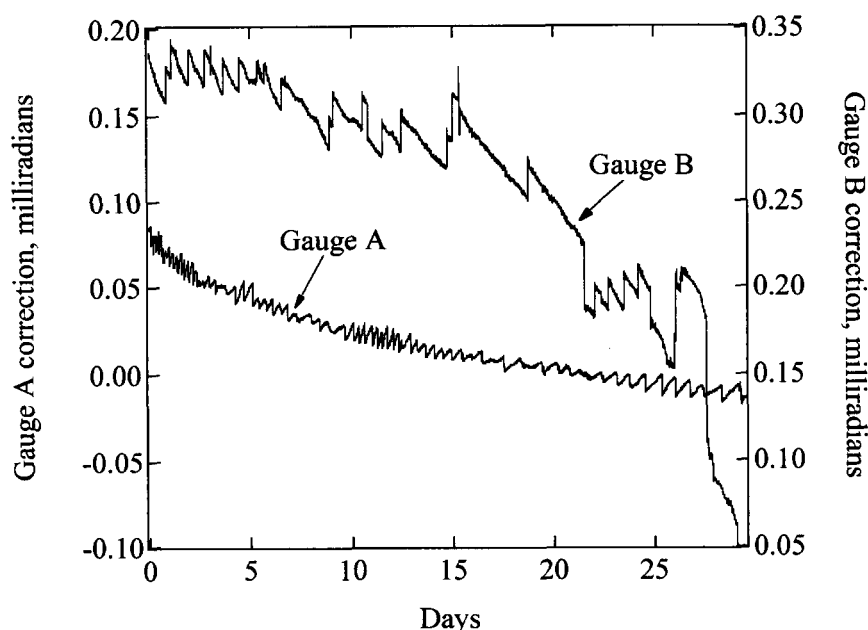


Fig. 7. Correction signal applied to metrology head steering mechanism. in the azimuthal (left-right) direction.

4. Other effects to look for

Table 1 lists the expected dominant effects that might appear near one and two cycles per day. The last two entries are the ether hypothesis that motivated the original Michelson-Morley experiment, and the idea that motivated this work.

Fig. 8 plots the data around the frequencies where these effects would be most easily observed. The effect at 1.93 cpd could be explained by lunar tides, but if that is the case, the effect of solar tides should also be seen at 2.0 cpd, although at $\sim 1/2$ the amplitude. None of the previously discussed diagnostics (temperatures, pointing) have frequency components at frequencies around 2 cpd, so no ready explanation for the peaks in fig. 8 is available, other than statistical fluctuations.

Finally, an anisotropy due to the sun's gravitational field would have appeared at 2.0 cpd. It can be ruled out at a level $dL/L \sim (0.1 \text{ nm})/(1 \text{ m}) = 10^{-10}$.

| Cause | Expected frequencies, cycles per day |
|---|--------------------------------------|
| Tidal effect of moon | 0.966, 1.932, ... |
| Tidal effect of sun | 1.0, 2.0, ... |
| Earth rotation-moon orbit coupling | 2.078 |
| Passage of earth through ether? (Sidereal day) | 1.0027, 2.0055, ... |
| Local G.R. anisotropy? | 2.0 |

Table 1. List of possible “non-technical” effects that would influence displacement metrology at frequencies near 1 and 2 cycles per day[12].

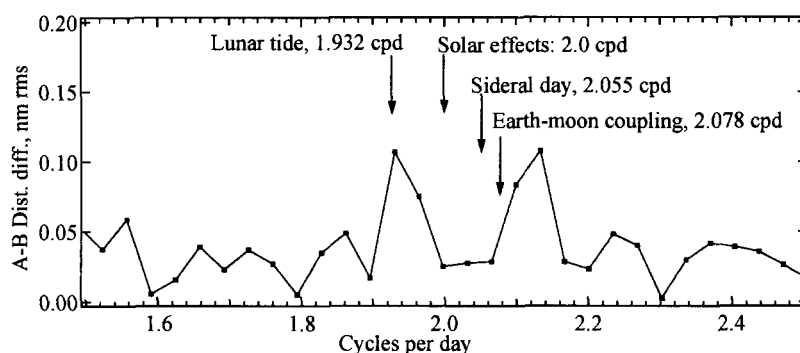


Fig. 8. Plot of A-B distance difference Fourier amplitudes, expanded around 2 cycles per day. Labels indicate the 2nd harmonic frequencies of various hypothetical effects listed in table 2.

III. Appendix: About SIM metrology

1. SIM metrology requirements

The Space Interferometry Mission (SIM) [13,14] will measure the angular positions of ~ 20000 astronomical objects (mainly stars) for the detection and characterization of planets, gravitational lensing events, black holes and other exotic phenomena. SIM will detect these by their influence on the angular

position of the object observed. For example, an earth-sized planet orbiting a nearby star at 1 AU could be detected by the angular “wobble” of the star, about 1 μ s (=4.8 picoradians).

SIM measures the relative angles of stars on the celestial hemisphere by observing two “guide” stars which determine the orientation of SIM itself, while the third, “science” star is measured. Each star’s angular position is measured by measuring the starlight phase delay between a pair of telescopes joined in an interferometer. Hence to function, SIM needs three starlight interferometers. (A fourth is available for redundancy.)

- Metrology* is needed to
1. provide knowledge of the angles between each interferometer (called external metrology) and
 2. to provide internal calibration of the optical delay in the starlight interferometers (internal metrology).

Fig. 9 is a cut-away view showing the four stellar interferometers (two guide, and two science) and the external metrology beams that link them together in a three-dimensional virtual “truss” of positional information.

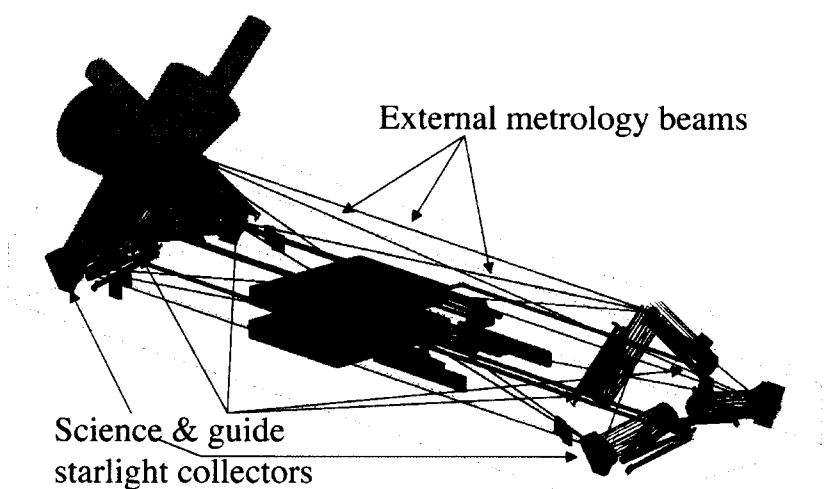


Fig. 9. SIM instrument layout. Blue indicates path of science starlight, green of guide starlight. Red indicates external metrology laser beams which measure distances between fiducials. The long dimension of the spacecraft is ~10 meters. Cones indicate the science and guide field-of-regard for the left side collectors. The right side field-of-regard cones, omitted for clarity, view the same portion of the sky.

The performance of SIM is directly related to the accuracy of the metrology. The error in measuring a star’s location is roughly $\epsilon(L)/D$ where $\epsilon(L)$ is the typical metrology error and $D=10$ meters is the baseline, the distance between the starlight interferometer telescopes. For an astrometric accuracy of 5 picoradians, we would need to limit errors to 50 pm. Because of other error sources, the contribution from metrology should actually be less than this.

| | Internal metrology requirement | External metrology requirement |
|---|--|------------------------------------|
| Number of gauges | 4 | 19 |
| Number of gauges for mission success* | 3 | 12 |
| Distance between fiducials | 20 m | Shortest: 2.5 m Longest: 10.6 m |
| Motion; ranges of distances | ~2.6 m | ~10 microns |
| Velocity, internal | 2 cm/s while changing stars, 1 micron/sec while observing | |
| Accuracy (absolute) | Not needed. | 3 microns rms |
| Accuracy relative | ~57 pm rms, 1 hour time scale; ~10 pm rms, 90 s time scale, <i>after removal of linear component**</i> | |
| Temp. coefficient | 2 pm/mK (soak); 50 pm/mK (sensitivity to gradients) | |
| * Assumes dispersed failures. Some failures are more tolerable than others. ** Modified observing schedule will allow off-line removal of drifts that are linear in time; further error removal based on instrument modeling should be possible. | | |

Table 2. SIM metrology requirements.

2. SIM metrology implementation

Displacement metrology for the SIM testbeds consists of a laser source [15] which supplies two $\lambda=1.3$ micron outputs with a small frequency difference F_{HET} which can be anywhere from 2 to 1000 kHz, the range of the phasemeter. The two frequency outputs serve as local oscillator (LO) and Probe sources. These outputs are carried to a metrology interferometer head (not to be confused with SIM's *starlight* interferometers) by polarization maintaining (PM) fibers. The final three meters use *polarizing* fiber to remove energy from the "wrong" (fast) polarization axis before reaching the interferometers. The "wrong" polarization would not contribute to the photodiode signal, and a different and unpredictable phase, especially given fiber-optic delivery of the laser light.

The interference signals from the interferometer, i.e. from the reference and measurement photodiodes, have a heterodyne frequency that is determined by the laser source (in this experiment, it was 2 kHz). The relative phase of the signals contains the distance information, and are measured by a phase measuring system [16,17] consisting of a sine-to-square wave converter and a digital averaging phasemeter. Averaging improves the effective resolution of the phasemeter. In this experiment, averaging for ten minutes per data point gave a resolution much better than a picometer.

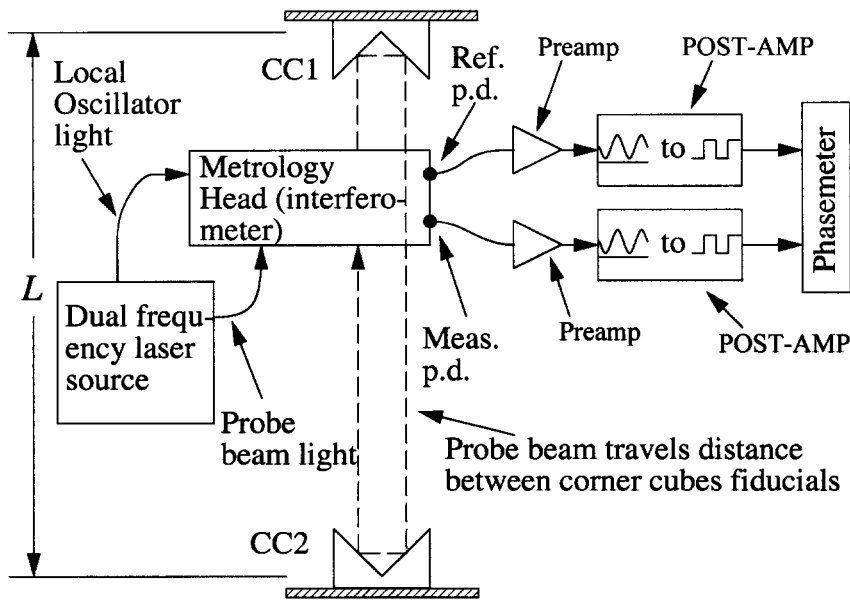


Fig. 10. Metrology gauge for measuring a single distance L . SIM uses 19 such gauges for external metrology and 4 for internal, starlight path, metrology. Two gauges were used for the anisotropy search.

Fig. 10 shows only one metrology gauge, but SIM will have 19 external gauges, which must work together to create a consistent three-dimensional shape, accurate to a few tens of picometers. The first step in showing that such a truss could be built was demonstrating close agreement between *pairs* of gauges. This is done in the Two-Gauge testbed [18], used in this experiment, with the result that the current gauges have:

1. cyclic non-linearity < 20 pm,
2. thermal sensitivity ~ 8 pm/mK,
3. drift ~ 300 pm/hour.

3. Prototype metrology interferometer head

The metrology interferometer [19,20] is shown in fig. 11 and 12. In this design, the probe beam is subdivided into an outer portion that travels between the fiducials and an inner portion that remains inside the head. These will form the Meas. and Ref. signals. Any leakage (diffraction and scattering could be causes) between inner and outer beams is a potential cause of cyclic nonlinearity. Masks have been added to reduce this leakage to acceptable levels.

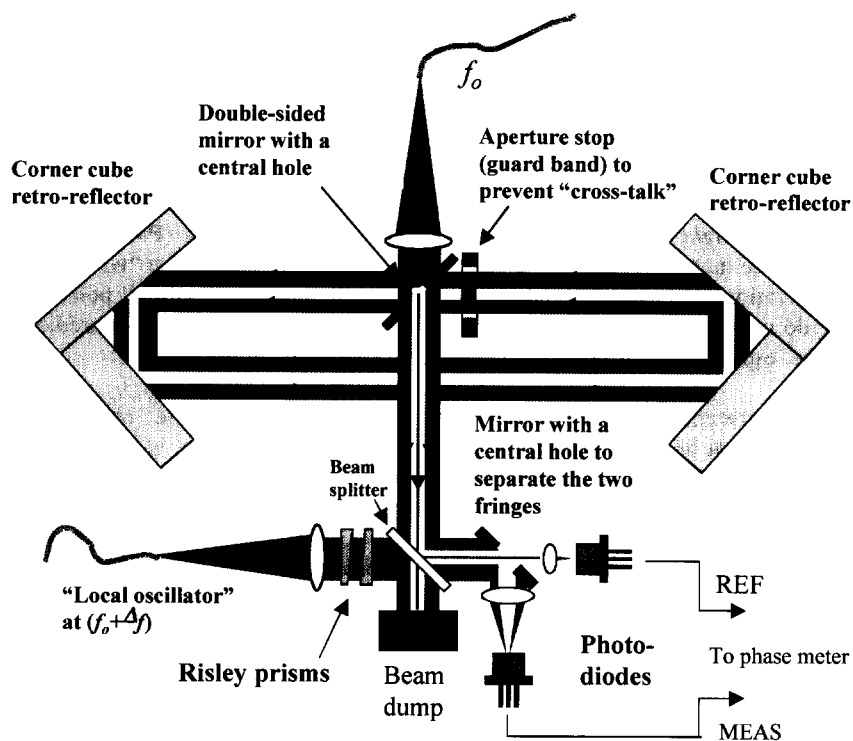


Fig. 11. Block diagram of metrology interferometer. The phase difference of the reference and measurement photodiode signals indicates the distance between corner cube fiducials.

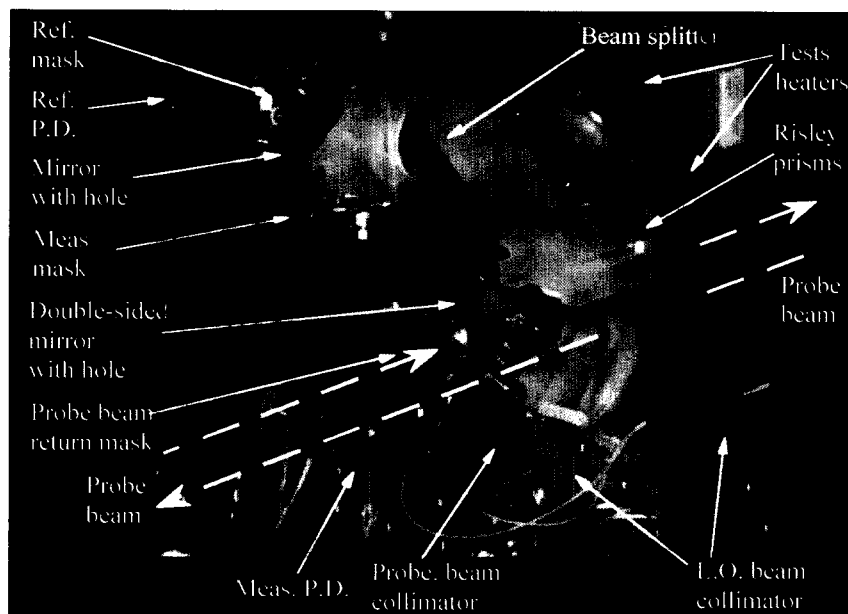


Fig. 12. Metrology head used in SIM testbeds. Heaters were placed on the rear and side surfaces of the zerodur bench supporting the optics to test thermal sensitivities.

4. Pointing control

For correct measurement of the distance L between corner cube retroreflector fiducials, the probe beam from a metrology head should be aimed parallel to the vector connecting the fiducials' vertices. Mispointing of the metrology head by an angle θ causes an error in the measured length

$$\varepsilon(L) = -L\theta^2/2.$$

For example, if $L = 10$ meters, and $\theta = 1 \mu\text{Radian}$, then the error will be $-5 \mu\text{m}$. Since the effect is quadratic, a small additional mispointing will quickly exceed the error budget, hence active alignment is essential. First demonstrated for single gauges [21], active alignment is used in the Two-Gauge testbed and has further evolved in KITE, the ongoing demonstration of a SIM-like metrology truss.

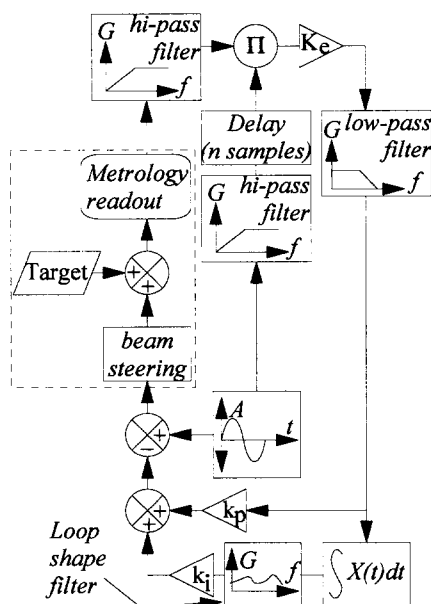


Fig. 13. Control loop for metrology head alignment. Two such loops, azimuth and elevation, are required per metrology head.

is a PI controller with some loop shaping for improved tracking. The lock-in amplifier dithering frequency is chosen such that measurement noise and structural dynamics are for the most part avoided. For these tests the dithering frequency was 2.2 Hz and the dither radius was 7 micro-radians.

5. Test environment (two-gauge facility)

The two-gauge facility can simultaneously test two prototype metrology heads (A and B). These are positioned between two corner cube fiducials and aligned such that the measurement beams are parallel to a line connecting the fiducials. (The heads are designed to allow each other's beam to pass through unimpeded.) The tank is evacuated and the measured inter-fiducial distance is monitored by the phase meter hardware and recorded by the computer system. In principle, the two gauges should agree exactly. Comparing the two gauges provides a sensitive test of the gauges' performance.

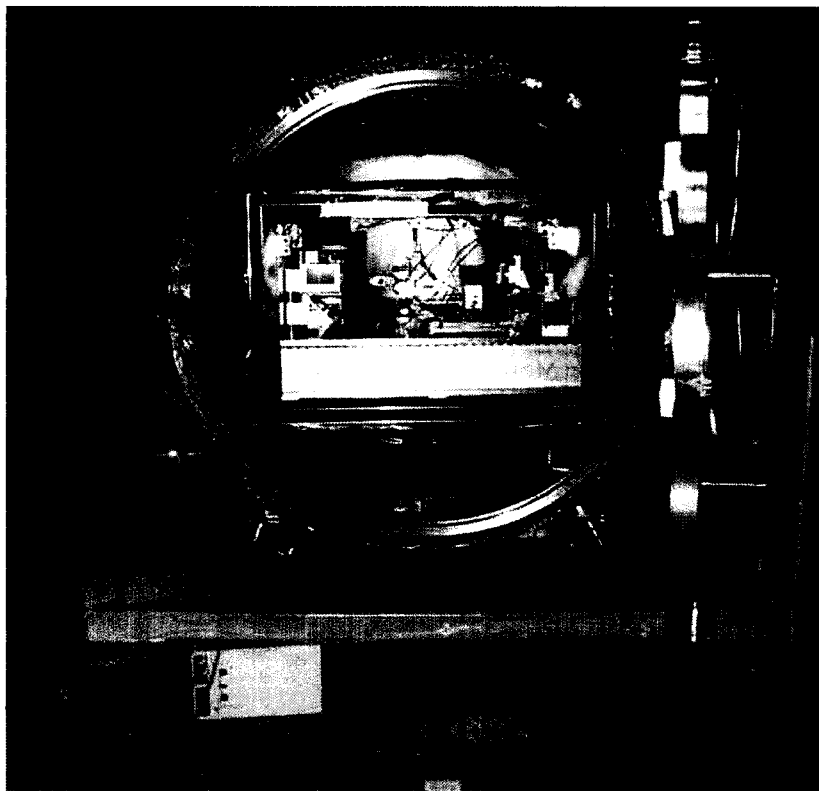


Fig. 14. Two gauge test facility, showing 122 cm diameter, 130 cm length, vacuum tank mounted on pneumatic vibration isolators.

To minimize thermal disturbances, the breadboard (which is in vacuum) is thermally isolated by a double shell of aluminum which is covered by multilayer insulation (gold colored foil). The vacuum tank itself is insulated and is actively held at a nearly constant temperature.

Fig. 13 shows the alignment control loop. The dashed box contains physical parts: piezoelectric (PZT) alignment actuators, metrology readout of L , and the target which is the instantaneous vector connecting the retroreflectors. The target moves due to external influences such as mechanical drift, but more importantly for SIM, because of slewing of the siderostat mirrors to acquire various stars.

The pointing system consists of a 2 degree of freedom (azimuth and elevation) PZT steering actuator, a lock-in amplifier based pointing error sensor with delay compensation, and a control law designed to track linear drift. Fig. 13 shows the control loop for one degree of freedom only. The control law

6. Acknowledgement

This research was carried out at the Jet Propulsion Laboratory, California Institute of Technology, under a contract with the National Aeronautics and Space Administration.

1. A. Hirai, H. Matsumoto, "Remote calibration of end standards using a low-coherence tandem interferometer with an optical fiber," *Optics Communications* **215** 1-3 pp 25-30 (2003)
2. personal communication: Y. Tomozawa, University of Michigan, 2002.
3. http://planetquest.jpl.nasa.gov/SIM/sim_index.html
4. SIM, *Taking the Measure of the Universe* JPL publication 400-811 3/99 (Available online at <http://sim.jpl.nasa.gov/library/book.html>)
5. L.L.Ames *et al.*, "SIM external metrology beam launcher (QP) development" in *Interferometry in Space*; Michael Shao; Ed., Proc. SPIE Vol. 4852, 347-354 (2003)
6. P.G. Halverson, L.S. Azevedo, R.T. Diaz, R.E. Spero, "Characterization of Picometer Repeatability Displacement Metrology Gauges" in *ODIMAP III, 3rd Topical Meeting on Optoelectronic Distance/Displacement Measurements and Applications*, Univ. of Pavia, Italy, 63-68 (2001).
7. J E Logan, P G Halverson, M W Regehr and R E Spero, "Automatic alignment of a displacement-measuring heterodyne interferometer," *Appl. Opt.* **41**, 4314-4317 (2002)
8. H. Muller, S. Herrmann, C. Braxmaier, S. Schiller, A. Peters, "Modern Michelson-Morley experiment using optical resonators," *Phys. Rev. Lett.* **91**, 020401 (2003).
9. <http://www.exphy.uni-duesseldorf.de/ResearchInst/FundPhys.html>
10. I. I. Shapiro *et al.*, "Radar Verification of the Doppler Formula", *Phys. Rev. Lett.* **17**, 17, (1966).
11. For an introduction to G.R. effects: *Exploring Black Holes*, E. F. Taylor and J. A. Wheeler. Addison Wesley Pub., 2000.
12. J. G. Williams, JPL, personal communication (2003).
13. SIM, *Taking the Measure of the Universe*, JPL publication 400-811 3/99. (Available online at sim.jpl.nasa.gov/library/book.html)
14. Laskin R.A., SIM Technology Development Overview: Light at the End of the Tunnel, *Interferometry in Space, Proceedings of the SPIE*, V. 4852, 16-32, 2003.
15. Dubovitsky S., Seidel D., Liu D., and Gutierrez R., Metrology source for high-resolution heterodyne interferometer laser gauges, *Proceedings of SPIE conference on Astronomical Interferometry*, V. 3350, 571-587, 1998.
16. Halverson, P.G., Loya, F.M.. Signal processing for order 10 pm accuracy displacement metrology gauges in real-world scientific applications, , *Proceedings of ICSO 2004, 5th International Conference on Space Optics*, 3/30/2004, Toulouse, France.
17. Halverson P.G. et al., A Multichannel Averaging Phasemeter for Picometer Precision Laser Metrology, *Optical Engineering for Sensing and Nanotechnology (ICOSN '99)* conference, 16-18 June 1999, Yokohama, Japan, *Proceedings of the SPIE*, V.3740, pp 646-649
18. Halverson P.G., Azevedo L.S., Diaz R.T., Spero R.E., Characterization of picometer repeatability displacement metrology gauges, *Proceedings of Optoelectronic Distance/Displacement Measurements and Applications (ODIMAP II)*, 63-68, Pavia, Italy, 9/2001
19. Zhao F. et al., Development of Sub-nanometer Racetrack Laser Metrology for External Triangulation Measurement for the Space Interferometry Mission, *Proceedings of the Sixteenth Annual Meeting of the American Society for Precision Engineering*, Nov. 10-15 2001, Arlington Virginia, pp 349-352.
20. Ames L.L. et al., SIM external metrology beam launcher (QP) development, *Interferometry in Space, Proceedings of the SPIE*, V. 4852, 347-354, 2003.
21. Logan J.E. et al., Automatic Alignment of a Displacement-Measuring Heterodyne Interferometer, *Applied Optics*, V. 41, 21 Page 4314-4317, 2002